

Detectability of the choroid plexus of the third ventricle with magnetic resonance ventriculography.

Ken Sato¹, Masanori Awaji¹, Shoichi Inagawa¹, Yuichiro Yoneoka², Junichi Yoshimura³, Norihiko Yoshimura¹, Hidefumi Aoyama¹

¹ Department of Radiology and Radiation Oncology, Niigata University Graduate School of Medical and Dental Sciences, 1-757 Asahimati-dori, Chuo-ku, Niigata-shi, Niigata 951-8510, Japan

² Department of Neurosurgery, Uonuma Institute of Community Medicine, Niigata University Medical and Dental Hospital, 4132 Urasa, Uonuma-shi, Niigata 949-7302, Japan

³ Department of Neurosurgery, Nagano Red Cross Hospital, 5-22-1 Wakasato, Nagano-shi, Nagano 380-8582, Japan

Corresponding author: Ken Sato

e-mail: ken.sato.1qaz2wsx@gmail.com telephone number: 81-25-227-2315

Ethical Statement:

All procedures performed in studies involving human participants were in accordance with the ethical standards of the institutional and/or national research committee and with the 1964 Helsinki declaration and its later amendments or comparable ethical standards.

Information concerning grants:

No funding was received for this study.

Conflict of Interest:

The authors declare that they have no conflict of interest.

The type of manuscript:

Original article

The word count of the text:

4182 words

Abstract

Purpose To clarify the detectability of the choroid plexus of the third ventricle (ChP13V) with magnetic resonance ventriculography (MRVn) employing a steady-state free precession (SSFP) sequence in comparison to surgical endoscopic movies as a golden standard, as we encountered some clinical cases of total agenesis of corpus callosum (ACC) where we could not recognize the choroid plexus of the third ventricle and found no previous article addressing this problem.

Materials and methods This retrospective study included consecutive patients from 2010 to 2016 for whom endoscopic evaluation of the third ventricle was conducted. The anterior portion of the right and left streaks of ChP13V was evaluated in 8 patients on 16 sites, while the posterior portion of both streaks of ChP13V was evaluated in 13 patients on 26 sites. Sensitivity of MRVn to visualize ChP13V with endoscopic movies as the golden standard was calculated.

Results Sensitivity of MRVn in visualizing the anterior portion of ChP13V was 0.813, and that for the posterior portion 0.692. The anterior portion of ChP13V was visualized in all cases where no tumor contacted the foramen of Monro.

Conclusion MRVn visualizes the anterior portion of ChP13V with significant sensitivity and the posterior portion with lower one.

Keywords choroid plexus, the third ventricle, magnetic resonance imaging (MRI)

Introduction

In the recent clinical experience, we encountered some cases of total agenesis of corpus callosum (ACC) where we could not point out existence of the choroid plexus of the third ventricle (ChP13V). No previous article on coincidence of ACC and absent ChP13V was found in the literature. One article contained two cases of ACC where a trace of ChP13V was illustrated in the figures [1]. In ontogeny of human beings, the primordium of ChP13V appears on the border of telencephalon and diencephalon by the end of the 2nd month of intrauterine life after the choroid plexus of the fourth ventricle and those of the lateral ventricles appear [2, 3], while some fibers of the prospective corpus callosum begin to penetrate the cellular bed of massa commissuralis in the primordium hippocampi at 10-12 weeks of fertilization age [1, 4]. Adding this temporal order of development and the reported two cases mentioned above to our experience, it seems reasonable to suppose that agenesis of ChP13V or some event closely related to it may lead to ACC. In order to address this hypothesis, we would like to evaluate the frequency of absence of ChP13V in cases of ACC using magnetic resonance imaging (MRI). To take on this task, we need some evidence that MRI can depict ChP13V, but have not found any article which dealt with this problem, though the choroid plexus of the lateral ventricles and that of fourth ventricle are well evaluated using MRI [5]. Steady-state free precession (SSFP) sequences depict minute structures with high spatial resolution and clear contrast against the cerebrospinal fluid [6-12] and has been routinely applied in our institution for patients with pathologies within or around the third ventricle before surgery. Here we retrospectively collected data of patients who had some disease within or around the third ventricle and undertook endoscopic surgery to determine if MR ventriculography (MRVn) employing a SSFP sequence visualizes ChP13V in comparison to surgical endoscopic movies as a golden standard.

Materials and Methods

Patient selection:

This retrospective study was approved by our institutional review board. The registry of neurosurgical operations maintained by the department of neurosurgery in our institution was consulted to extract consecutive patients from January 1, 2010 to May 31, 2016 for whom either 1) transsphenoidal resection of a pituitary adenoma or a craniopharyngioma with extension into the third ventricle was done with assistance of endoscopy (group A) or 2) frontal craniotomy and endoscopy of the third ventricle was conducted for third-ventriculostomy or biopsy/resection of a tumor in the wall of the third ventricle (group B). For each cohort, endoscopic movies were reviewed and patients with endoscopic visualization of the proper sites suitable to identify the anterior or posterior portion of the right and left streaks of ChP13V were selected as subjects for this retrospective study. The proper sites suitable to identify the anterior portion of the right and left streaks of ChP13V were supposed to be the anterior part of the roof of the third ventricle in the proximity of the foramen of Monro and the proper sites suitable to identify the posterior portion of

the right and left streaks of ChPI3V to be the posterior part of the roof of the third ventricle in the proximity of the suprapineal recess.

It was found that MRVn employing a SSFP sequence with or without gadolinium enhancement for the third ventricle was performed preoperatively within a month before the endoscopic procedure for all the patients in groups A and B as it was one of the routine sequences of preoperative MRI for lesions around the third ventricle in our institution.

Protocol of MRVn:

Data were obtained with five 1.5 to 3 Tesla MRI machines as follow, using a SSFP sequence with its denomination in a respective parenthesis; Philips Achieva 1.5T (3D Balanced-Fast Field Echo (3D FFE)), Philips Ingenia 1.5T (3D Balanced-FFE), Siemens MAGNETOM Verio 3T (3D constructive interference in steady state (3D CISS)), GE Signa HDxt 1.5T (3D fast imaging employing steady-state acquisition (3D FIESTA)), GE DISCOVERY MR750w 3.0T (3D fast imaging employing steady-state acquisition-phase cycling (3D FIESTA-C)).

The parameters are as follow.

Three 1.5 Tesla MRI machines; TR = 5.5 - 5.8 msec, TE = 2.2 - 2.8 msec, flip angle = 70°, FOV = 120 × 120 - 120 × 126 mm, matrix = 160 - 256 × 256 - 285, pixel size = 0.47 - 0.75 × 0.42 - 0.49 mm, slice thickness = 0.8 - 1.0 mm, slice interval = 0.5 - 0.8 mm, acquisition time = 1 min 39 sec, 1 min 59 sec, 3 min 15 sec, band width = 325.8 Hz/pixel (GE Signa HDxt 1.5T), water fat shift = 0.303 - 0.32 pixel (Philips Achieva 1.5T/ Ingenia 1.5T)

Two 3 Tesla MRI machines; TR = 5.6 - 5.8 msec, TE = 2.3 - 2.4 msec, flip angle = 33° - 40°, FOV = 120 × 120 - 120 × 126 mm, matrix = 192 - 256 × 256, pixel size = 0.47 - 0.63 × 0.47 - 0.49 mm, slice thickness = 0.8 - 1.0 mm, slice interval = 0.5 - 0.8 mm, acquisition time = 2 min 52 sec, 3 min 31 sec, band width = 476 - 520.9 Hz/pixel

Slice orientation; In group A, MRVn images were acquired in coronal and axial planes for all the patients. In group B, the images were acquired in coronal and axial planes for one patient and in sagittal planes for the others.

Evaluation of the endoscopic movies:

For each of group A and B, endoscopic movies were retrospectively analyzed by a neurosurgeon and a neuroradiologist to evaluate the existence and the size of the anterior or posterior portion of the right and left streaks of ChPI3V in a graded scale; large, small, or not recognized. The images of MRVn were blinded to the evaluators. The final decision in evaluation was made by the neurosurgeon in case of disagreement. For cases where the anterior or posterior portion of the right and left streaks of ChPI3V was recognized, static images was generated from the movies for comparison at the final stage of the evaluation of MRVn images as described later.

Evaluation of MRVn:

Three months after the evaluation of the endoscopic movies, MRVn images were evaluated by two neuroradiologists with 22 and 11 years of experience (rater a, b) respectively and one radiologist in his late year of residency (rater c) using a medical display terminal of a picture archiving and communication system (PACS) (FUJIFILM Medical Systems, U.S.A, Inc , SYNAPSE EX-V version 1.11). The endoscopic movies as well as its result of the evaluation were blinded to the evaluators of MRVn. MRVn images were reviewed in all the three major orthogonal planes, after images in one or two major orthogonal planes not obtained in the original acquisition was reconstructed with data obtained in the other planes in the original acquisition on a PACS terminal by each of the evaluators. In MRVn images, ChP13V was judged to be recognized when all the following three conditions were met; 1) it is a long and fine structure extending posteriorly from the foramen of Monro on the roof of the third ventricle, 2) at a closer look, the long and fine structure seems to be an assemblage of minute granules, 3) it is not a simple tube or thread so that the internal cerebral vein or any vessel is not wrongly judged to be a choroid plexus.

The existence and the size of the anterior or posterior portion of the right and left streaks of ChP13V was evaluated in a graded scale; recognized, possibly recognized, or not recognized. The final conjoint decision in evaluation was made by the largest number of evaluators sharing the same opinion in case of disagreement. If the three votes were equally distributed among the three alternative scales, it was judged as possibly recognized.

After the final decision, the three evaluators collectively discerned if the localization of each anterior or posterior portion of the right and left streaks of ChP13V recognized by themselves in the images of MRVn corresponds correctly to the site observed in the endoscopic images captured from the movies.

Statistics:

The inter-rater reliability between three evaluators for the triple grading evaluation of MRVn was tested in terms of Spearman's rank correlation coefficient (ρ) and Kendall's coefficient of concordance (W) using SPSS Statistics version 24.0.0.0 (IBM Inc.). P value less than 0.05 was supposed statistically significant. Sensitivity of MRVn to visualize ChP13V in comparison to the endoscopic movies as a golden standard was calculated after dichotomization of the alternatives: "large" and "small" were grouped together as "recognized" and contrasted to "not recognized" in endoscopic evaluation and "recognized" and "possibly recognized" were grouped together as "recognized" and contrasted to "not recognized" in evaluation of MRVn.

Result

For group A, 15 candidate patients were retrieved from the registry of the department of neurosurgery, and those with visualization of the bilateral proper sites in the endoscopic movies to identify the anterior portion

of the right and left streaks of ChPI3V were selected to make a subject group of eight patients with 16 proper sites for this study. The proper sites to identify the posterior portion of the right or left streaks of ChPI3V was not observed in the endoscopic movies in this group. For group B, 21 candidate patients were retrieved from the registry, and those with visualization of the bilateral proper sites in endoscopic movies to identify the posterior portion of the right and left streaks of ChPI3V were selected to make a subject group of 13 patients with 26 proper sites for this study. The proper sites to identify the anterior portion of the right or left streaks of ChPI3V was not observed in the endoscopic movies in this group.

In summary, eight patients with 16 proper sites for evaluation of the anterior portion of the right and left streaks of ChPI3V and 13 patients with 26 proper sites for evaluation of the posterior portion of the right and left streaks of ChPI3V were included in this study.

Patient characteristics:

Among eight patients in Group A, four were male and four female; four with pituitary adenoma, four with craniopharyngioma (Table 1). Among 13 patients in Group B, six were male and seven female; 10 patients of hydrocephalus due to Blake's pouch cyst in two patients, tectal glioma in four, non-neoplastic aqueductal stenosis in two, medulloblastoma in one, and cavernous hemangioma in one, and three patients with a tumor in the wall of the third ventricle comprising one with germinoma, one with pineal parenchymal tumor of intermediate differentiation, and one with craniopharyngioma. The mean age of patients is 52.9 years [range 6 - 77 years] in Group A, and 26.2 years [range 1 - 67 years] in Group B. In group A, seven cases were imaged with contrast-enhanced MRVn and one case with non-contrast MRVn. In group B, seven cases were imaged with contrast-enhanced MRVn and six cases with non-contrast MRVn.

Result of the endoscopic evaluation:

The existence of the anterior portion of the right and left streaks of ChPI3V was confirmed on all the proper sites in all the patients of the group A and the existence of the posterior portion of the right and left streaks of ChPI3V was confirmed on all the proper sites in all the patients of the group B (Table 2). In group A, it was judged large on five sites and small on 11 sites in the grading scale. In dichotomization for sensitivity analysis, "large" and "small" were grouped together into "recognized" for all the 16 sites in contrast to "not recognized" for no site. In group B, it was judged large on 4 sites, small on 22 sites in the grading scale. In dichotomization for sensitivity analysis, "large" and "small" were grouped together into "recognized" for all the 26 sites in contrast to "not recognized" for no site.

Result of the evaluation of MRVn:

Evaluation by each of the three raters and the final conjoint decision in evaluation of MRVn in both group A and B is shown in comparison to the evaluation of endoscopic movies in Table 2. In group A, the anterior portion of the right or left streaks of ChPI3V was recognized on 13 sites, possibly recognized on no site,

and not recognized on three sites. In dichotomization for sensitivity analysis, “recognized” and “possibly recognized” were grouped together into “recognized” for 13 sites in contrast to “not recognized” for three sites. The collective inspection found that the localization by the evaluators of each anterior portion of the right and left streaks of ChPI3V recognized or possibly recognized in the images of MRVn corresponded correctly to the site observed in the endoscopic images captured from the movies (Fig. 1a, 1b). Also found was that a tumor reached the foramen of Monro in the MRVn on all the three sites where ChPI3V was not recognized. In group B, the posterior portion of the right or left streaks of ChPI3V was recognized on eight sites, possibly recognized on 10 sites, and not recognized on eight sites. In dichotomization for sensitivity analysis, “recognized” and “possibly recognized” were grouped together into “recognized” for 18 sites in contrast to “not recognized” for eight sites. The localization of every posterior portion of the right and left streaks of ChPI3V recognized or possibly recognized in the images of MRVn corresponded correctly to the site observed in the endoscopic images captured from the movies (Fig. 2a, 2b).

Result of the statistical analysis:

In group A, Spearman’s rank correlation coefficients (ρ) in the triple grading evaluation of MRVn of the anterior portion of ChPI3V for each pair of the three evaluators were 0.787 (between rater a and b, $P < 0.001$), 0.894 (between rater a and c, $P < 0.001$), 0.704 (between rater b and c, $P = 0.002$) and Kendall’s coefficient of concordance (W) was 0.857 ($P = 0.001$). The inter-rater reliability among the three evaluators was significantly high.

In group B, Spearman’s rank correlation coefficients (ρ) in the triple grading evaluation of MRVn of the posterior portion of ChPI3V for each pair of the three evaluators were 0.321 (between rater a and b, $P = 0.109$), -0.330 (between rater a and c, $P = 0.875$), 0.431 (between rater b and c, $P = 0.028$) and Kendall’s coefficient of concordance (W) was 0.497 ($P = 0.054$). The inter-rater reliability between rater b and c in the evaluation of MRVn was significantly high, though the other pairs including rater a failed to show significant reliability.

Sensitivity of MRVn to visualize the anterior portion of ChPI3V in comparison to the endoscopic movies was 0.813, and that to visualize the posterior portion 0.692 (Table 3).

Specificity could not be obtained due to the lack of a case where ChPI3V was not observed in the endoscopic movies; in other words, the existence of the anterior or posterior portion of the right and left streaks of ChPI3V was confirmed in all cases with the endoscopic movies. In this consequence, specificity cannot be obtained and accuracy is equal to sensitivity.

Discussion

In this study, sensitivity of MRVn to visualize the anterior portions of ChPI3V with the endoscopic movies as the golden standard was high and that for the posterior portion of ChPI3V was moderate.

The inter-rater reliability among the three evaluators for the anterior portion of ChPI3V was high and

significant, while that for the posterior portion of ChPI3V was modest. One of the reasons for this difference may lie in that the anterior portion of ChPI3V near the foramen of Monro is directly connected to the plexus of the lateral ventricle and easy to identify and that the anterior portion near the foramen of Monro can be larger in size than the posterior portion in some cases as one may see in a literature of cadaveric anatomy for surgical exploration of the lateral and third ventricles [13]. This size difference may be reflected in the result of the endoscopic evaluation in this study that the anterior portion of ChPI3V was evaluated as large on five of all the 16 sites (31%) while the posterior portion as large on four out of all the 26 sites (15%) (Table 2). In group A, the anterior portions of ChPI3V was not recognized in MRVn on three sites of the total 16 sites, where the tumor reached the foramen of Monro in the MRVn images on all the three sites and may have hampered identification of ChPI3V (Fig. 3a, b). In group B, the posterior portion of the right or left streaks of ChPI3V was not recognized on eight sites of the total 26 sites, where a funicular structure was not visualized or lacked a granular appearance (Fig. 4a – c).

In this study to determine if MRVn visualizes ChPI3V, we used a SSFP which renders images with a submillimeter spatial resolution and was reported to visualize minute structures such as cranial nerves and an arachnoid cyst wall bordered with the cerebrospinal fluid better than the other sequences [6-12].

As a background of this study, we encountered in the recent clinical practice some cases of ACC where we could not point out existence of ChPI3V. No previous article on coincidence of ACC and absent ChPI3V was found in the literature. One article contained two cases of ACC where a trace of ChPI3V was illustrated in the figures [1].

ChPI3V comprises two longitudinal funicular structures running parallel in the anteroposterior direction on the midline of the luminal surface of the roof of the third ventricle and connecting with the corresponding right or left choroid plexus of the lateral ventricle through the foramina of Monro. It is shown to be smaller in general than those of the lateral ventricles in a cadaveric study [13].

In ontogeny of human beings, the primordium of ChPI3V appears on the border of telencephalon and diencephalon by the end of the 2nd month of intrauterine life after the choroid plexus of the fourth ventricle and those of the lateral ventricles appear [2]. A comprehensive atlas of normal human central nervous system development clearly illustrates that ChPI3V becomes recognized separately from the choroid plexus of the lateral ventricles by eight weeks of gestational age before the corpus callosum is formed [3]. Some fibers of the prospective corpus callosum begin to penetrate the cellular bed of massa comissuralis in the primordium hippocampi at 10-12 weeks of fertilization age [1, 4].

Adding this temporal order of development of ChPI3V and the corpus callosum and the reported two cases mentioned above to our experience, it seems reasonable to suppose that agenesis of ChPI3V or some event closely related to it may lead to ACC. In order to address this hypothesis, we wish to evaluate the frequency of absence of ChPI3V in cases of ACC. To take on this task, we need some evidence that MRI can visualize ChPI3V, but have not found any article which dealt with this problem, though the choroid plexus of the lateral ventricles and that of fourth ventricle are well evaluated using MRI [5]. With the result

of this study, we now think we can go further to evaluate the frequency of absence of ChPI3V in cases of ACC with MRI. It lies on its extension to clarify if the other anomalies of the midline structures of human telencephalon and diencephalon may be associated with absence of ChPI3V or not.

Beyond the problem of coincidence of absent ChPI3V and ACC as well as the other congenital midline anomalies, clinical impact of evaluating ChPI3V with MRI is unknown due to the unclear clinical significance of ChPI3V itself. Even the long believed role of the choroid plexus as the principal site of CSF production with active transport of ions and micronutrients was recently challenged by some researchers [14, 15], though is still supported by a substantial body of experimental and clinical data according to the others [16], and for the moment we take a hypothesis that the choroid plexus plays an important and integral, even if not the primary, role to produce CSF with homeostatic control of its ions and micronutrients so that the brain functions normally.

This study is retrospective in nature and carries limitations as follow. The number of the subjects was small. The evaluation of the size of ChPI3V in the endoscopic movies may be influenced by the distance from the tip of the endoscope to ChPI3V, though the evaluation on the existence of ChPI3V may not be affected significantly. MRVn was obtained with machines of different magnetic field strength, from 1.5 to 3 tesla, though the spatial resolution of MRVn with 1.5 Tesla was equivalent to that with 3 Tesla. The MRI machines were products of different vendors and the parameters for the pulse sequence somewhat differed in its consequence. Slice orientation and usage of contrast agent were diverse. Though no significant statistical difference in the final conjoint decisions of both group A and B was generated by the difference of magnetic field strength (3T vs 1.5T, $P = 0.841$), vendors (Philips vs Siemens vs GE, $P = 0.362$), MR pulse sequence (3D FFE vs 3D bFFE, $P = 0.238$; 3D FIESTA vs 3D FIESTA-C, $P = 0.808$), nor usage of contrast material (contrast-enhanced and non-contrast, $P = 0.864$), still remain those limitations as we remind ourselves to the small number of the subjects.

Conclusion

MRVn employing a SSFP sequence visualizes the anterior portion of ChPI3V with significant sensitivity and the posterior portion with lower one.

References

- 1) Loeser JD, Alvord EC Jr. Agenesis of the corpus callosum. *Brain*. 1968 Sep;91(3):553-70
- 2) Netsky MG, Shuangshoti S. I Origin of Choroid Plexus and Ependyma. In: Netsky MG, Shuangshoti S *The choroid plexus in health and disease*. John Wright and Sons Ltd., Bristol;1975. pp3-18
- 3) Shirley A. Bayer, Joseph Altman. *The Human Brain During the Early First Trimester*. 1st Edition In the Series: *Atlas of Human Central Nervous System Development*. CRC Press Florida: 2008, pp432-434 ISBN 9780849314247
- 4) Rakic P, Yakovlev PI. Development of the corpus callosum and cavum septi in man. *J Comp Neurol*.

- 1968 Jan;132(1):45-72. PubMed PMID: 5293999.
- 5) Madhukar M, Choudhary AK, Boal DK, Dias MS, Iantosca MR. Choroid plexus: normal size criteria on neuroimaging. *Surg Radiol Anat.* 2012;34:887-895
 - 6) Casselman JW, Kuhweide R, Deimling M, Ampe W, Dehaene I, Meeus L. Constructive interference in steady state-3DFT MR imaging of the inner ear and cerebellopontine angle. *AJNR Am J Neuroradiol.* 1993;14:47-57
 - 7) Aleman J, Jokura H, Higano S, Akabane A, Shirane R, Yoshimoto T. Value of constructive interference in steady-state three-dimensional, Fourier transformation magnetic resonance imaging for the neuroendoscopic treatment of hydrocephalus and intracranial cysts. *Neurosurgery* 2001 Jun;48(6):1291-5; discussion 1295-6
 - 8) Seitz J, Held P, Strotzer M, Volk M, Nitz WR, Dorenbeck U, et al. MR imaging of cranial nerve lesions using six different high-resolution T1-and T2(*)-weighted 3D and 2D sequences. *Acta Radiol* 2002 Jul;43(4):349-53
 - 9) M. Kocaoglu, N. Bulakbasi, T. Ucoz, B Ustunsoz, Y. Pabuscu, C, Tayfun, et al. Comparison of contrast-enhanced T1-weighted and 3D constructive interference in steady state images for predicting outcome after hearing-preservation surgery for vestibular schwannoma. *Neuroradiology* 2003; 45: 476-481
 - 10) Hatipoğlu HG, Durakoğlugil T, Ciliz D, Yüksel E. Comparison of FSE T2W and 3D FIESTA sequences in the evaluation of posterior fossa cranial nerves with MR cisternography. *Diagn Interv Radiol* 2007 Jun;13(2):56-60
 - 11) M. Awaji, K. Okamoto, K. Nishiyama. Magnetic resonance cisternography for preoperative evaluation of arachnoid cysts. *Neuroradiology.* 2007;49:721-726
 - 12) Jennifer Linn, M.D., Bernhard Moriggl, M.D., Friederike Schwarz, Thomas P. Naidich, M.D., Ph.D., Urs D. Schmid, M.D., Marthin Wiesmann, M.D., et al. Cisternal segments of the glossopharyngeal, vagus, and accessory nerves: detailed magnetic resonance imaging-demonstrated anatomy and neurovascular relationships. *J Nerosurg.* 2009;110:1026-1041
 - 13) Rhoton AL Jr. The lateral and third ventricles. *Neurosurgery.* 2002 Oct;51 (4 Suppl) :S207-71 (See Figure 5.12)
 - 14) Oresković D, Klarica M. The formation of cerebrospinal fluid: nearly a hundred years of interpretations and misinterpretations. *Brain Res Rev.* 2010 Sep 24;64(2):241-62
<https://doi.org/10.1016/j.brainresrev.2010.04.006>
 - 15) Orešković D, Radoš M, Klarica M. Role of choroid plexus in cerebrospinal fluid hydrodynamics. *Neuroscience.* 2017 Jun 23;354:69-87 <https://doi.org/10.1016/j.neuroscience.2017.04.025>
 - 16) Spector R, Robert Snodgrass S, Johanson CE. A balanced view of the cerebrospinal fluid composition and functions: Focus on adult humans. *Exp Neurol.*2015 Nov;273:57-68
<https://doi.org/10.1016/j.expneurol.2015.07.027>

Figure Captions

Fig. 1 a An endoscopic image captured from the movie of the anterior portion of ChPI3V eyed from the bottom of the third ventricle in a patient of craniopharyngioma (patient 4 in the group A). The right and left streaks of the choroid plexus were observed in the third ventricle near the foramen of Monro with connection to their counterpart of the lateral ventricles: the anterior portion of ChPI3V was judged as large on both of the right and left sides. **b** A coronal image of preoperative MRVn (Siemens / MAGNETOM Verio 3T / 3D CISS) employing a SSFP sequence of the same patient shows the anterior portion of the right and left streaks of ChPI3V near the foramen of Monro with continuation from their counterpart of the lateral ventricles

Fig. 2 a An endoscopic image captured from the movie of the posterior portion of ChPI3V eyed from the anterior portion of the third ventricle in a patient of cystic craniopharyngioma upwardly compressing the floor of the third ventricle (patient 8 in the group B). The right and left streaks of ChPI3V are recognized on the roof of the third ventricle near the suprapineal recess: the posterior portion of ChPI3V was judged as large on both of the right and left sides. **b** A coronal image of preoperative MRVn (Philips / Ingenia 1.5T / 3D Balanced-FFE) employing a SSFP sequence of the same patient shows the posterior portion of the right and left streaks of ChPI3V on the roof of third ventricle near the suprapineal recess

Fig. 3 a An endoscopic image captured from the movie of the anterior portion of ChPI3V eyed from the bottom of the third ventricle in a patient of pituitary adenoma (patient 5 in the group A). The image was taken after removal of the tumor. The right and left streaks of the anterior portion of the choroid plexus were observed in the third ventricle near the foramen of Monro with connection to their counterpart of the lateral ventricles and both were judged as small. **b** A coronal image of preoperative MRVn (Siemens / MAGNETOM Verio 3T / 3D CISS) employing a SSFP sequence of the same patient. The tumor reached the foramen of Monro. For recognition of the anterior portion of ChPI3V in the MRVn, rater a/b/c evaluated respectively as not recognized/partially recognized/not recognized for each right and left streaks and conjointly judged as not recognized, though another look with generous criteria may evaluate it as recognized.

Fig. 4 a An endoscopic image captured from the movie of the posterior portion of ChPI3V eyed from the anterior portion of the third ventricle in a patient of hydrocephalus due to Blake's pouch cyst (patient 1 in the group B). The right and left streaks of ChPI3V are recognized on the roof of the third ventricle near the suprapineal recess and both were judged as small. **b, c** Coronal and left sagittal images of preoperative MRVn (Philips / Achieva 1.5T / 3D FFE) employing a SSFP sequence of the same patient. The coronal image **b** was a section near the suprapineal recess indicated as a dashed line in the images **c**. For recognition of the posterior portion of ChPI3V in the MRVn, rater a/b/c evaluated respectively as not recognized/partially recognized/partially recognized for the left streak and conjointly judged as partially recognized, while rater a/b/c evaluated respectively as not recognized/not recognized/partially recognized for the right streak and conjointly judged as not recognized. The posterior portion of the left streak of

ChP13V barely showed a granular appearance in the sagittal image c, while the posterior portion of the right streak was not clearly identified.

Table 1 Patient characteristics

	group A	group B	P value
Number of patients	8	13	
Sex (male/female)	4/4	6/7	0.92
Mean age [range](years)	52.9 [range 6-77]	26.2 [range 1-67]	0.02
MRVn (CE/non-CE)	7/1	7/6	0.12
disorder	4 pituitary adenoma 4 craniopharyngioma	10 hydrocephalus due to; 2 Blake's pouch cyst 4 tectal glioma 2 non-neoplastic aqueductal stenosis 1 medulloblastoma 1 cavernous hemangioma 1 germinoma 1 pineal parenchymal tumor of intermediate differentiation 1 craniopharyngioma	

CE; Contrast-enhanced

Table 2 Evaluation of MRVn in comparison to endoscopic movies in both group A and B

patient	left streak of ChPl3V						right streak of ChPl3V				
	evaluation of MRVn			final conjoint decision	evaluation of endoscopic images	evaluation of MRVn			evaluation of endoscopic images		
	rater					rater					
	a	b	c			a	b	c			
group A (anterior portion of ChPl3V)	1	R	R	R	R	large	R	R	R	R	large
	2	R	R	PR	R	small	R	R	R	R	small
	3	R	R	R	R	small	R	R	R	R	small
	4	R	R	R	R	large	R	R	R	R	large
	5	N	PR	N	N	small	N	PR	N	N	small
	6	R	R	R	R	small	R	R	R	R	large
	7	R	R	R	R	small	N	R	N	N	small
	8	R	R	R	R	small	R	R	R	R	small
group B (posterior portion of ChPl3V)	1	N	PR	PR	PR	small	N	N	PR	N	small
	2	N	R	R	R	small	N	R	PR	PR	small
	3	R	R	PR	R	small	R	R	PR	R	small
	4	R	N	R	R	small	N	N	PR	N	small
	5	N	N	N	N	small	N	N	N	N	small
	6	N	N	N	N	small	N	N	N	N	small
	7	R	R	PR	R	small	R	R	N	R	small
	8	PR	R	PR	PR	large	PR	R	PR	PR	large
	9	R	PR	PR	PR	large	R	PR	N	PR	large
	10	N	R	R	R	small	N	R	PR	PR	small
	11	N	PR	R	PR	small	N	PR	R	PR	small
	12	N	R	R	R	small	N	R	PR	PR	small
	13	N	N	N	N	small	N	N	N	N	small

R = recognized, PR = possibly recognized, N = not recognized

rater a = neuroradiologist with 22 years of experience, b = neuroradiologist with 11 years of experience, c = radiologist

Table 3 Sensitivity of MRVn

group A		final conjoint decision of MRVn		sensitivity
		R	N	
evaluation of endoscopic images	R	13	3	0.813
	N	0	0	

group B		final conjoint decision of MRVn		sensitivity
		R	N	
evaluation of endoscopic images	R	18	8	0.692
	N	0	0	

R = recognized, N = not recognized

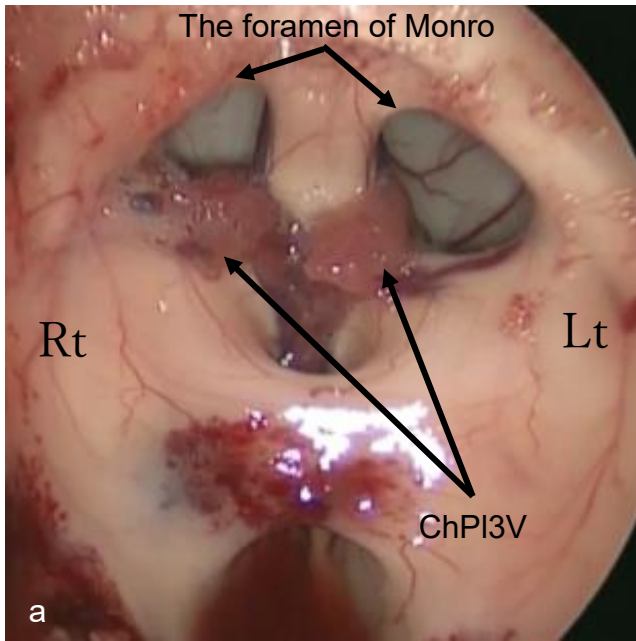


Fig. 1a

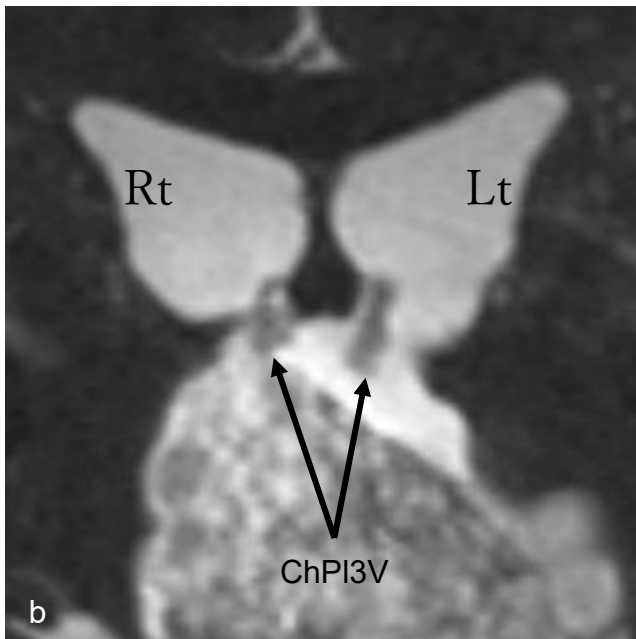


Fig. 1b

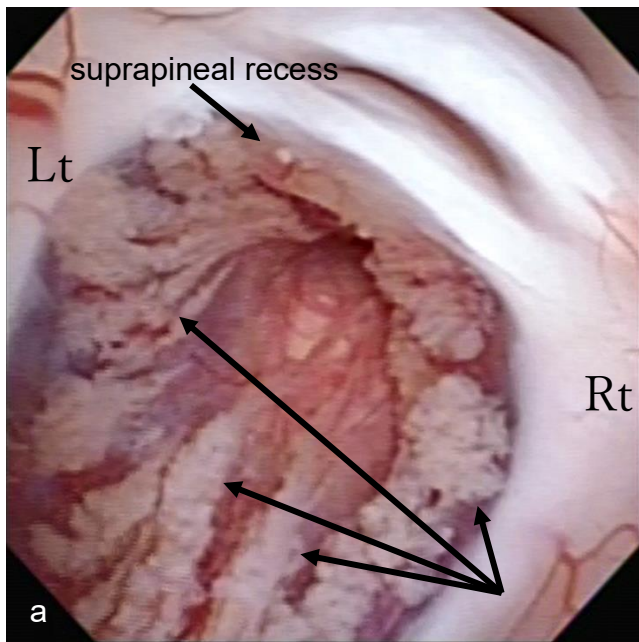


Fig. 2a

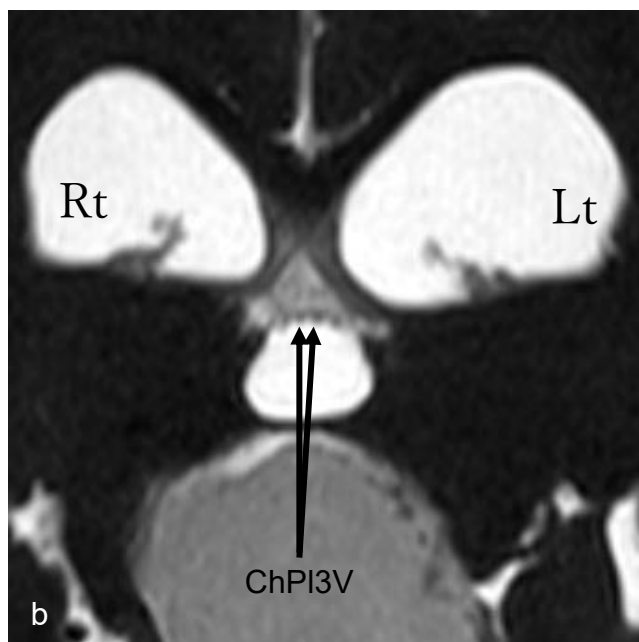


Fig. 2b

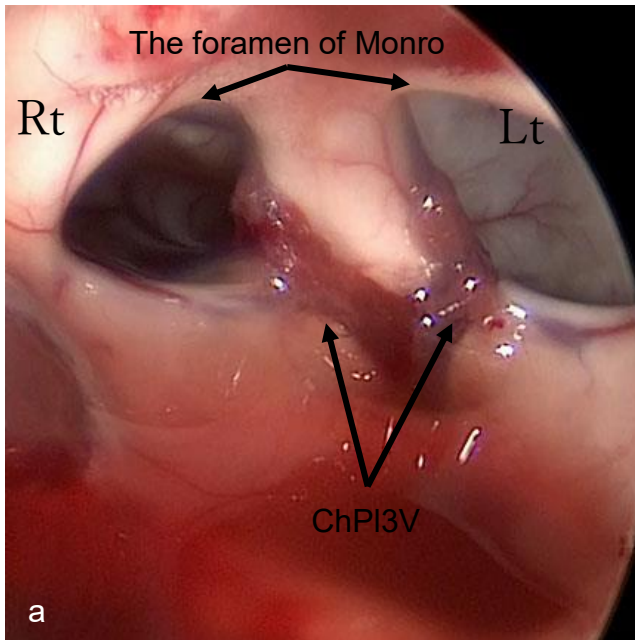


Fig. 3a

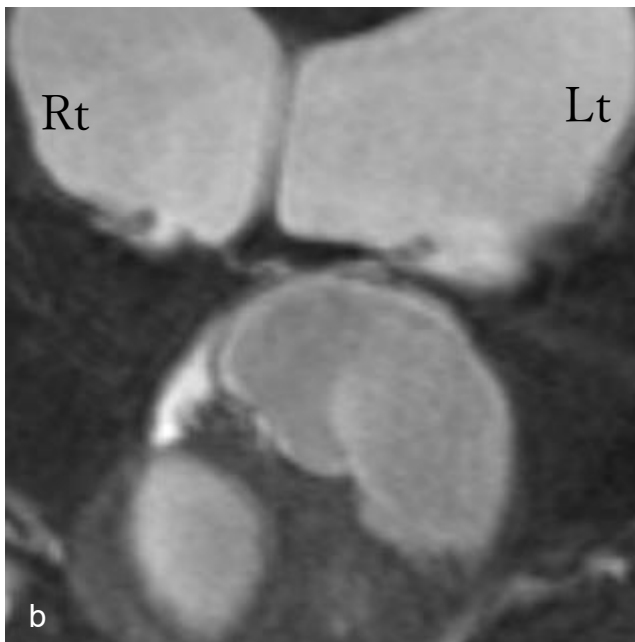


Fig. 3b

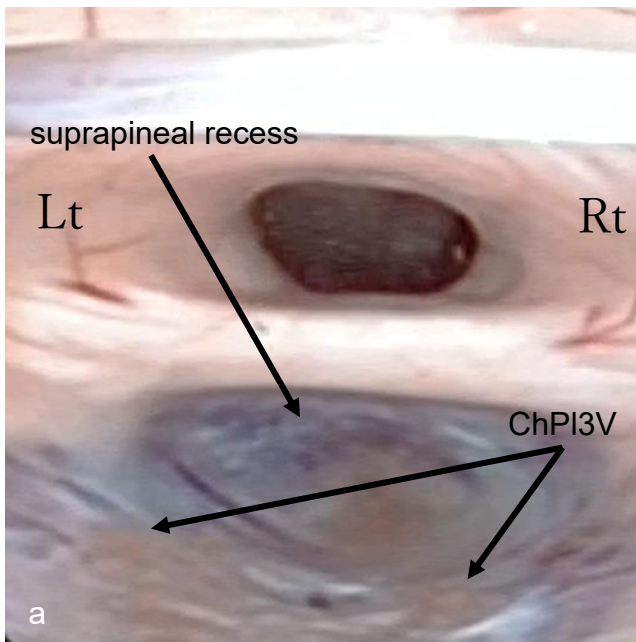


Fig. 4a

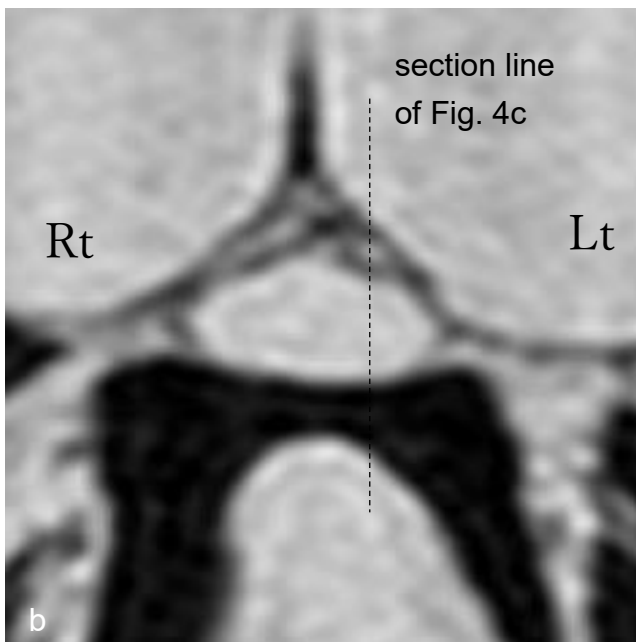


Fig. 4b

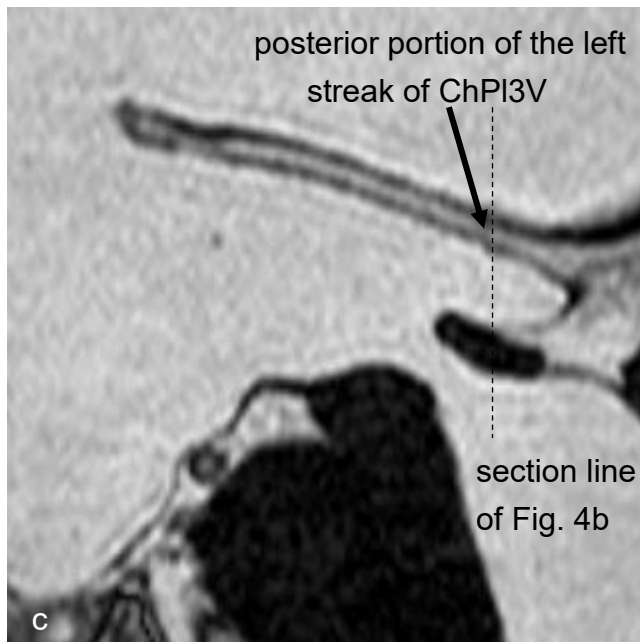


Fig. 4c